

Molecule Design on Isoxazolone-based Derivatives with Large Second-order Harmonic Generation Effect for Terahertz Wave Generation

Xinyuan Zhang,^{a, d} Xingxing Jiang,^{a, d} Pengxiang Liu,^{b, c} Yin Li,^a Heng Tu,^a
Zheshuai Lin,^a Degang Xu,^b Guochun Zhang,^{* a} Yicheng Wu^a and Jianquan
Yao^b

^aBeijing Center for Crystal Research and Development, Key Laboratory of Functional Crystals and Laser Technology, Technical Institute of Physics and Chemistry, Chinese Academy of Sciences, Beijing 100190, China. Email: gczhang@mail.ipc.ac.cn

^bThe Institute of Laser & Optoelectronics, College of Precision Instruments and Optoelectronics Engineering, Tianjin University, Tianjin 300072, China

^cThe Key Laboratory of Weak-Light Nonlinear Photonics, Ministry of Education, School of Physics and TEDA Applied Physics Institute, Nankai University, Tianjin 300071, China

^dUniversity of Chinese Academy of Sciences, Beijing 100049, PR China

Content

Experimental details

Crystal structures

Figure S1. ORTEP drawing of (a) PDI, (b) PTI, (c) PFI, and (d) PMI-(I) molecule in the crystalline state (Prob = 50).

Figure S2. TGA-DSC curve of the (a) PDI, (b) PTI, (c) PFI, and (d) PMI-(I) crystals.

Figure S3. The obtained crystals by slow evaporation method: (a) PDI crystal from acetonitrile; (b) PTI crystal from chloroform; (c) PFI crystal from chloroform; (d) PMI-(I) crystal from acetone.

Figure S4. Schematic diagram of the experimental setup for THz DFG with MLS crystals.

Figure S5. Geometrical structure in PDI crystal.

Figure S6. Hydrogen bonds and π - π interactions in PDI crystals (green line for hydrogen bonds and purple line for π - π interactions).

Figure S7. Geometrical structure in PTI crystal and spatial stacking pattern of PTI molecules (purple line for π - π interactions).

Figure S8. Hydrogen bonds in PTI crystals.

Figure S9. Geometrical structure in a PFI crystal and spatial stacking pattern of PFI molecules.

Figure S10. π - π interactions in PFI crystals (purple line).

Figure S11. Geometrical structure in PMI-(I) crystal.

Figure S12. Hydrogen bonds and π - π interactions in PMI-(I) crystal (green line for

hydrogen bonds and purple line for π - π interactions).

Table S1 Crystallographic data and structure refinements for the 3-phenyl-5-isoxazolone-based crystals.

Table S2 Crystallographic data and structure refinements for the 3-methyl-5-isoxazolone-based crystals.

Table S3. Thermal properties including melting point (T_m) and initial weight-loss temperature (T_i) of BPMI, DBPI, DPPI, and PMI-(II).

Table S4. Hydrogen bonds for PDI [\AA and deg.].

Table S5. Hydrogen bonds for PTI [\AA and deg.].

Table S6. Hydrogen bonds for PMI-(I) [\AA and deg.].

Experiments

(Z)-3-phenyl-4-(4-(pyrrolidin-1-yl)benzylidene)isoxazol-5(4H)-one (PDI)

¹H NMR (400 MHz, CDCl₃) δ 8.39 (d, *J* = 7.5 Hz, 2H), 7.60 – 7.51 (m, 5H), 7.37 (s, 1H), 6.59 (d, *J* = 9.1 Hz, 2H), 3.47 (t, *J* = 6.6 Hz, 4H), 2.11 – 2.06 (m, 4H).

(Z)-4-((5-methylthiophen-2-yl)methylene)-3-phenylisoxazol-5(4H)-one (PTI)

¹H NMR (400 MHz, CDCl₃) δ 7.82 (d, *J* = 3.8 Hz, 1H), 7.67 (s, 1H), 7.62 – 7.55 (m, 5H), 6.97 (d, *J* = 3.8 Hz, 1H), 2.65 (s, 3H).

(Z)-4-((9H-fluoren-2-yl)methylene)-3-phenylisoxazol-5(4H)-one (PFI)

¹H NMR (400 MHz, CDCl₃) δ 8.77 (s, 1H), 8.27 (d, *J* = 8.1 Hz, 1H), 7.88 (dd, *J* = 9.0, 5.8 Hz, 2H), 7.67 (s, 1H), 7.61 (tdd, *J* = 6.8, 4.5, 2.1 Hz, 6H), 7.45 – 7.42 (m, 2H), 4.01 (s, 2H).

(Z)-4-(4-(methylthio)benzylidene)-3-phenylisoxazol-5(4H)-one (PMI)

¹H NMR (400 MHz, CDCl₃) δ 8.30 (d, *J* = 8.6 Hz, 2H), 7.62 – 7.54 (m, 5H), 7.51 (s, 1H), 7.30 (d, *J* = 8.6 Hz, 2H), 2.55 (s, 3H).

(Z)-4-([1,1'-biphenyl]-4-ylmethylene)-3-phenylisoxazol-5(4H)-one (PBMI)

¹H NMR (400 MHz, CDCl₃) δ 8.43 (d, *J* = 8.4 Hz, 2H), 7.76 (d, *J* = 8.4 Hz, 2H), 7.68 – 7.56 (m, 8H), 7.49 (t, *J* = 7.4 Hz, 2H), 7.43 (t, *J* = 7.2 Hz, 1H).

(Z)-4-(3,4-dimethoxybenzylidene)-3-phenylisoxazol-5(4H)-one (PDBI)

¹H NMR (400 MHz, CDCl₃) δ 8.74 (d, *J* = 2.0 Hz, 1H), 7.60 – 7.55 (m, 6H), 7.50 (s, 1H), 6.93 (d, *J* = 8.5 Hz, 1H), 4.02 (s, 3H), 3.99 (s, 3H).

(Z)-4-(4-(diphenylamino)benzylidene)-3-phenylisoxazol-5(4H)-one (PDPI)

¹H NMR (400 MHz, CDCl₃) δ 8.29 (d, *J* = 9.0 Hz, 2H), 7.61 (dd, *J* = 7.2, 2.4 Hz, 2H),

7.57 (d, $J = 7.2$ Hz, 3H), 7.43 (s, 1H), 7.39 (d, $J = 8.0$ Hz, 4H), 7.23 (t, $J = 6.8$ Hz, 6H), 6.97 (d, $J = 9.1$ Hz, 2H).

(Z)-3-methyl-4-(4-(pyrrolidin-1-yl)benzylidene)isoxazol-5(4H)-one (MDI)

^1H NMR (400 MHz, CDCl_3) δ 8.41 (d, $J = 8.1$ Hz, 2H), 7.20 (s, 1H), 6.59 (s, 2H), 3.46 (d, $J = 6.7$ Hz, 4H), 2.24 (s, 3H), 2.08 (dd, $J = 6.2, 3.1$ Hz, 4H).

(Z)-3-methyl-4-((5-methylthiophen-2-yl)methylene)isoxazol-5(4H)-one (MTI)

^1H NMR (400 MHz, CDCl_3) δ 7.88 (d, $J = 3.8$ Hz, 1H), 7.49 (s, 1H), 6.97 (d, $J = 3.9$ Hz, 1H), 2.64 (s, 3H), 2.27 (s, 3H).

(Z)-4-((9H-fluoren-2-yl)methylene)-3-methylisoxazol-5(4H)-one (MFI)

^1H NMR (400 MHz, CDCl_3) δ 8.81 (s, 1H), 8.28 (d, $J = 8.1$ Hz, 1H), 7.92 – 7.86 (m, 2H), 7.63 – 7.60 (m, 1H), 7.48 (s, 1H), 7.45 – 7.41 (m, 2H), 4.01 (s, 2H), 2.32 (s, 3H).

(Z)-3-methyl-4-(4-(methylthio)benzylidene)isoxazol-5(4H)-one (MMI)

^1H NMR (400 MHz, CDCl_3) δ 8.31 (d, $J = 8.6$ Hz, 2H), 7.31 (d, $J = 6.2$ Hz, 2H), 7.29 (s, 1H), 2.55 (s, 3H), 2.28 (s, 3H).

(Z)-4-(4-(dimethylamino)benzylidene)-3-methylisoxazol-5(4H)-one (MAI)

^1H NMR (400 MHz, CDCl_3) δ 8.41 (d, $J = 8.8$ Hz, 2H), 7.22 (s, 1H), 6.74 (d, $J = 9.1$ Hz, 2H), 3.16 (s, 6H), 2.25 (s, 3H).

(Z)-4-(4-methoxybenzylidene)-3-methylisoxazol-5(4H)-one (MBI)

^1H NMR (400 MHz, CDCl_3) δ 8.43 (s, 2H), 7.34 (s, 1H), 7.01 (d, $J = 8.9$ Hz, 2H), 3.92 (s, 3H), 2.28 (s, 3H).

Crystal structures

The ORTEP drawing of PDI, PTI, PFI, and PMI-(I) molecules in crystalline state were shown in **Figure S1**. The molecule conformations of the four acentric crystals are slightly different. In PDI, the heterocyclic ring plane and the benzene plane (C(1)-C(6)) that connected by double bond is in an angle of 13°. The angle between the heterocyclic ring and the benzene plane (C(11)-C(26)) that connected directly is about 56° (as seen in **Figure S1(a)**). In PTI, the heterocyclic ring plane and the thiophenyl plane connected by double bond is nearly in the same plane in an angle about 6°. The angle between the heterocyclic ring and the benzene plane (C(9)-C(14)) is about 52° (as seen in **Figure S1(b)**). In PFI, the heterocyclic ring plane and the fluorenyl plane (C(1)-C(13)) connected by alkene is merely in an angle about 7°, and the angle between the heterocyclic ring and the benzene plane (C(18)-C(23)) that connected directly is about 60° (as seen in **Figure S1(c)**). In PMI-(I), the heterocyclic ring plane and the phenyl plane (C(1)-C(6)) are nearly in the same plane in an angle about 7°. The angle between the heterocyclic ring and the benzene plane (C(11)-C(16)) that connected directly is about 58° (as seen in **Figure S1(d)**). Obviously, PDI, PTI, PFI, and PMI-(I) all possess a non-main plane phenyl ring on the heterocyclic ring and show high planarity between the electron donor and the electron acceptor, which provides an effective approach for electron transfer.

According to crystallographic data, the PDI crystal crystallizes in the noncentrosymmetric orthorhombic space group $Pna2_1$ and point group $mm2$. The molecule structure and crystal packing diagrams of the PDI are shown in **Figure S5**.

The angle between neighboring PDI molecules along *a*-axis is 115°, while PDI molecules along *b*-axis are parallel. Along *c*-axis, the angle between the adjacent PDI molecules with same head-tail orientation is 36.2°, and the centroid distance between the adjacent molecules is 10.4 Å. Molecular interactions originated from π - π interactions and hydrogen bonds (**Table S4**) in PDI crystal structure are shown in **Figure S6**. One of the π - π interactions exists between the heterocyclic ring and the phenyl ring C(11)-C(16) along *a*-axis with centroid distance of 3.70 Å, and another interaction is between the heterocyclic ring and the phenyl ring (C(1)-C(6)) along *b*-axis with centroid distances of 3.62 Å.

PTI crystal belongs to the noncentrosymmetric monoclinic space group *Pc* and point group *m*. The molecule structure and crystal packing diagrams of the PTI are shown in **Figure S7**. The neighboring molecules along *a*-axis and *b*-axis are parallel. The neighboring molecule planes along *c*-axis are in the angle of 65.5°. Along *c*-axis, the main molecular interactions between unparallel molecules of the PTI crystal are medium strong hydrogen bonds (**Table S5**) as seen in Figure S6. There are also π - π interactions in the crystal (seen in **Figure S8**). One is between the heterocyclic ring and the thiophene ring along *b*-axis with centroid distance of 3.60 Å, and another is between the heterocyclic ring and the phenyl ring along *c*-axis with distance of 3.64 Å.

PFI crystal belongs to the noncentrosymmetric monoclinic space group *Cc* and point group *m*. The molecule structure and crystal packing diagrams of the PFI molecules are shown in **Figure S9**. Crystallographic data reveals that the neighboring molecules planes along the *c*-axis are in angle of 105°, and the molecules along *a*-axis

and *b*-axis are in parallel arrangement. Molecular interactions in PFI crystal are quite simple, as seen in **Figure S10**. The main molecular interactions π - π interactions are along *b*-axis and *c*-axis. The distance between the heterocyclic ring and the phenyl ring (C(8)-C(13)) along *b*-axis is 3.57 Å, and the distance between the heterocyclic ring and the phenyl ring (C(18)-C(23)) along *c*-axis is 3.61 Å.

PMI-(I) crystal also belongs to the noncentrosymmetric monoclinic space group *Cc* and point group *m*. The molecule structure and crystal packing diagrams of the PMI-(I) are shown in **Figure S11**. The adjacent molecules along *a*-axis and *b*-axis are parallel. The neighboring molecules planes along the *c*-axis are in the angle of 73.4°. Molecular interactions in PMI-(I) crystal are also quite simple, as seen in **Figure S12**. The main molecular interactions in each layer along *c*-axis are weak hydrogen bonds (**Table S6**) of O(2)...H(6)-C(6) between neighboring molecules. The π - π interactions are along *b*-axis and *c*-axis, the distance between the heterocyclic ring and the phenyl ring C(1)-C(6) and C(11)-C(16) are both 3.53 Å.

Figure S1. ORTEP drawing of (a) PDI, (b) PTI, (c) PFI, and (d) PMI-(I) molecule in the crystalline state (Prob = 50).

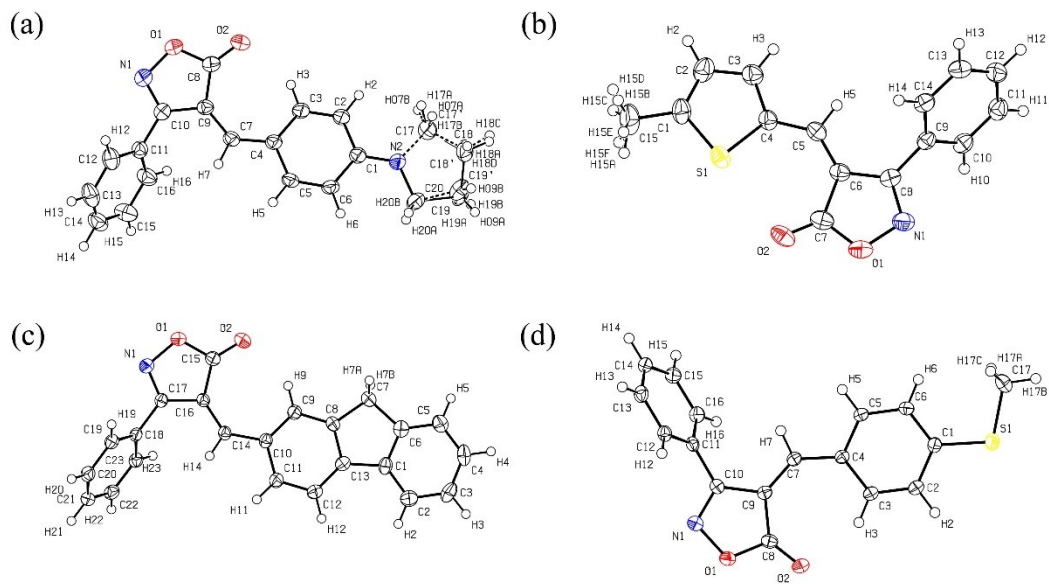


Figure S2. TGA-DSC curve of the four crystals.

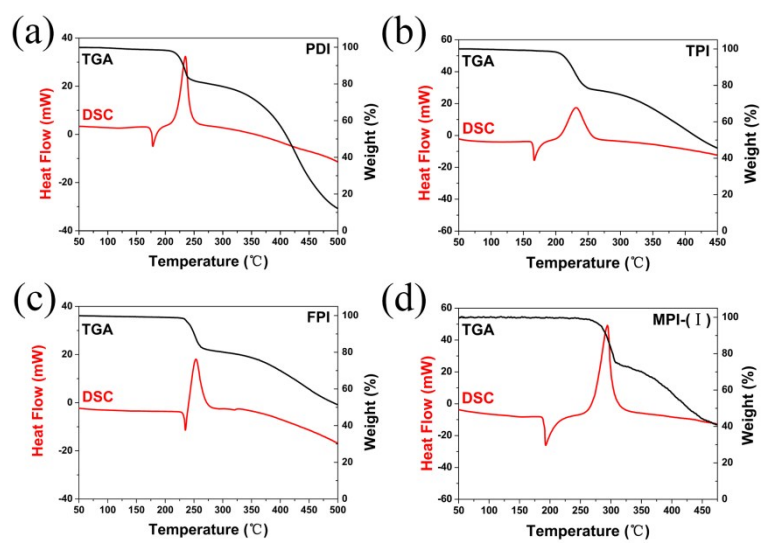


Figure S3. The obtained crystals by slow evaporation method: (a) PDI crystal from acetonitrile; (b) PTI crystal from chloroform; (c) PFI crystal from chloroform; (d) PMI-(I) crystal from acetone.

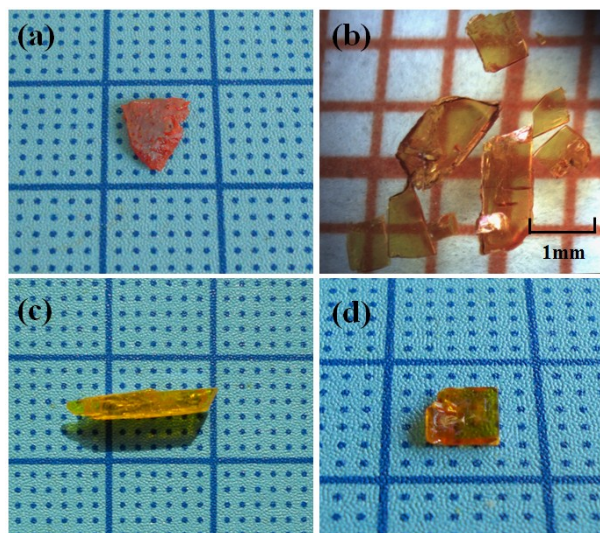


Figure S4. Schematic diagram of the experimental setup for THz DFG with MLS crystals.

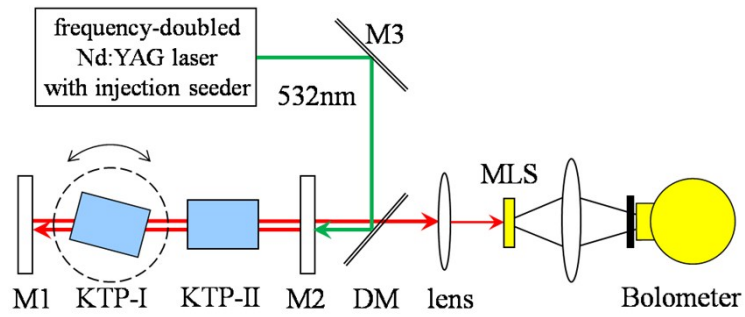


Figure S5. Geometrical structure in PDI crystal.

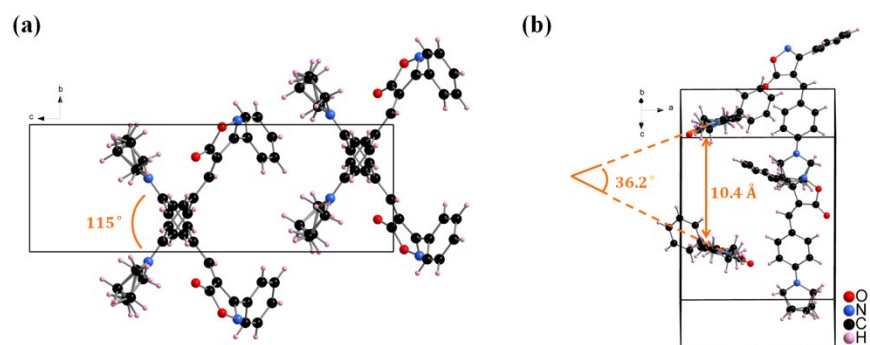


Figure S6. Hydrogen bonds and π - π interactions in PDI crystals (green line for hydrogen bonds and purple line for π - π interactions).

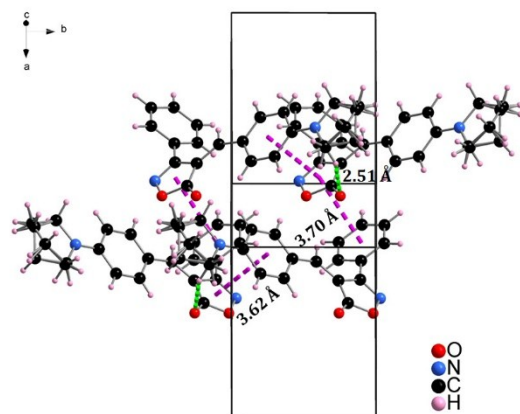


Figure S7. Geometrical structure in PTI crystal and spatial stacking pattern of PTI molecules (purple line for π - π interactions).

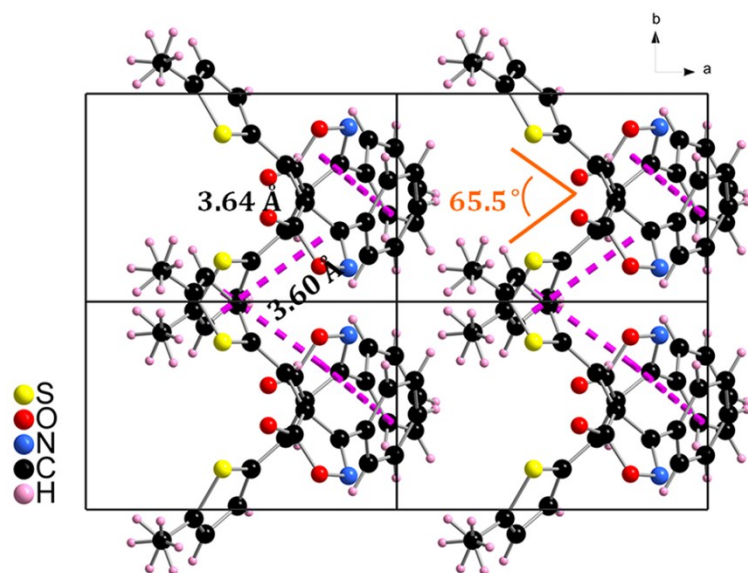


Figure S8. Hydrogen bonds in PTI crystals.

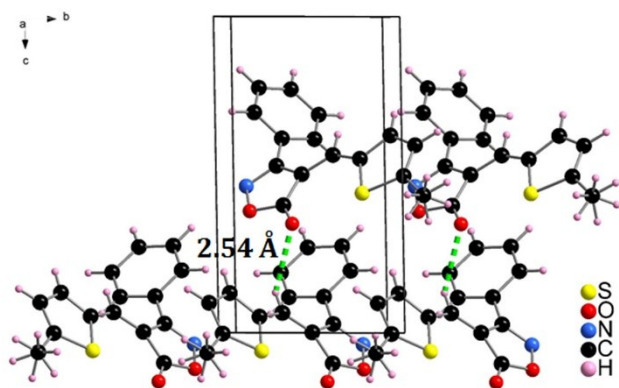


Figure S9. Geometrical structure in a PFI crystal and spatial stacking pattern of PFI molecules.

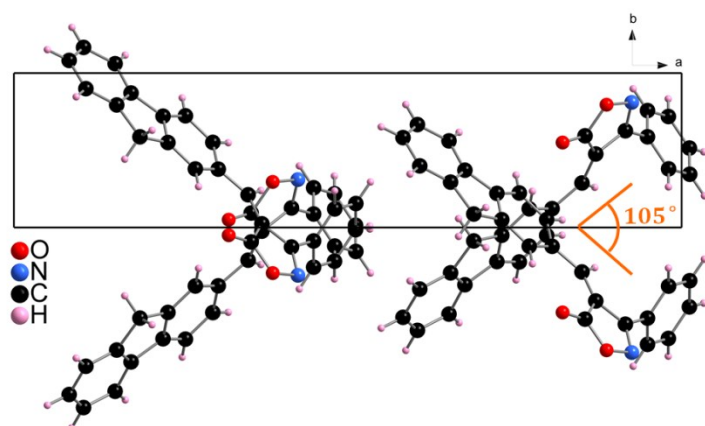


Figure S10. π - π interactions in PFI crystals (purple line).

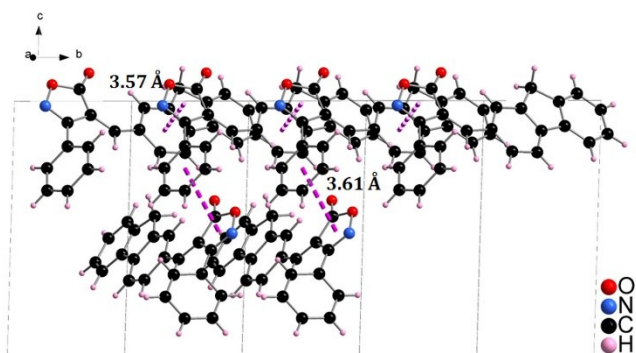


Figure S11. Geometrical structure in PMI-(I) crystal.

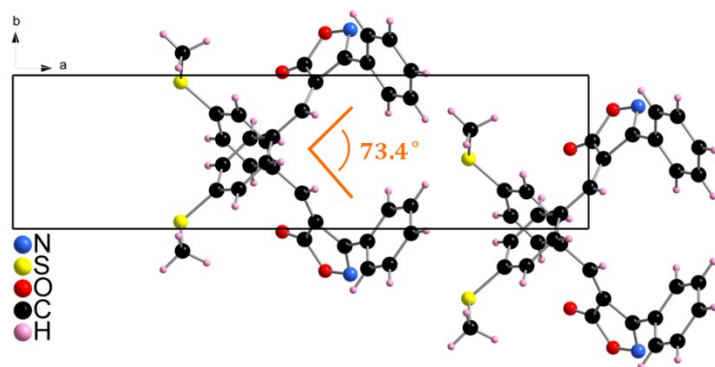


Figure S12. Hydrogen bonds and π - π interactions in PMI-(I) crystal (green line for hydrogen bonds and purple line for π - π interactions).

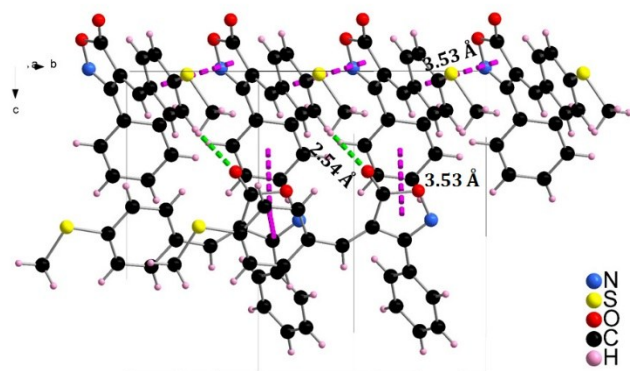


Table S1. Crystallographic data and structure refinements for the 3-phenyl-5-isoxazolone-based crystals.

	PDI	PTI	PFI	PMI-(I)	DLS ^[25]	MLS ^[25]
formula	C ₂₀ H ₁₈ N ₂ O ₂	C ₁₅ H ₁₁ NO ₂ S	C ₂₃ H ₁₅ NO ₂	C ₁₇ H ₁₃ NO ₂ S	C ₁₈ H ₁₆ N ₂ O ₂	C ₁₇ H ₁₃ NO ₃
fw	318.36	269.31	337.36	295.34	292.33	279.28
crystal system	Orthorhombic	Monoclinic	Monoclinic	Monoclinic	Monoclinic	Orthorhombic
space group	<i>Pna2</i> ₁	<i>Pc</i>	<i>Cc</i>	<i>Cc</i>	<i>Cc</i>	<i>Pna2</i> ₁
<i>a</i> (Å)	12.040(3)	9.466(3)	24.442(8)	20.924(6)	21.112(11)	11.482(3)
<i>b</i> (Å)	6.7907(14)	6.060(2)	5.6023(19)	5.5952(16)	6.525(3)	6.0114(13)
<i>c</i> (Å)	19.562(4)	11.771(5)	11.966(4)	11.691(3)	12.163(6)	19.382(5)
<i>α</i> (deg)	90	90.00	90	90	90.00	90.00
<i>β</i> (deg)	90	106.248(5)	97.638(3)	90.568(4)	119.582(5)	90.00
<i>γ</i> (deg)	90	90.00	90	90	90.00	90.00
<i>V</i> (Å ³)	1599.4(6)	648.3(4)	1624.0(10)	1368.6(7)	1457.1(12)	1337.8(5)
<i>Z</i>	4	2	4	4	4	4
<i>R</i> ₁ (> 2σ(<i>I</i>))	0.0447	0.0330	0.0478	0.0368	0.0397	0.0375
w <i>R</i> ₂ (all data)	0.0967	0.0631	0.1111	0.0858	0.0906	0.0891
CCDC No.	1448252	1448258	1448255	1448256	947161	1055698

	PBMI	PDBI	PDPI	PMI-(II)
formula	C ₂₂ H ₁₅ NO ₂	C ₁₈ H ₁₅ NO ₄	C ₂₈ H ₂₀ N ₂ O ₂	C ₁₇ H ₁₃ NO ₂ S
fw	325.35	309.31	416.46	295.34
crystal system	Monoclinic	Monoclinic	Orthorhombic	Monoclinic
space group	<i>P2₁/c</i>	<i>P2₁/c</i>	<i>Pbca</i>	<i>P2₁/c</i>
<i>a</i> (Å)	24.695(7)	7.339(2)	11.550(2)	41.870(11)
<i>b</i> (Å)	5.6676(15)	19.964(6)	11.294(2)	5.7143(13)
<i>c</i> (Å)	11.644(3)	10.771(3)	33.009(6)	11.597(3)
<i>α</i> (deg)	90	90	90	90
<i>β</i> (deg)	96.552(4)	104.306(5)	90	96.235(4)
<i>γ</i> (deg)	90	90	90	90
<i>V</i> (Å ³)	1619.1(8)	1529.2(8)	4305.9(13)	2758.3(12)
<i>Z</i>	4	4	8	8
<i>R</i> ₁ (> 2σ(<i>I</i>))	0.0549	0.0578	0.0451	0.0597
wR ₂ (all data)	0.1289	0.14	0.1273	0.1701
CCDC No.	1448267	1448251	1448253	1448257

Table S2 Crystallographic data and structure refinements for the 3-methyl-5-isoxazolone-based crystals.

	MDI	MTI	MFI	MMI	MAI	MBI
formula	C ₁₅ H ₁₆ N ₂ O ₂	C ₁₀ H ₉ NO ₂ S	C ₁₈ H ₁₃ NO ₂	C ₁₂ H ₁₁ NO ₂ S	C ₁₃ H ₁₄ N ₂ O ₂	C ₁₂ H ₁₁ NO ₃
fw	256.30	207.24	275.29	233.28	230.26	217.22
crystal system	Monoclinic	Monoclinic	Triclinic	Monoclinic	Monoclinic	Monoclinic
space group	<i>P</i> 2 ₁ / <i>c</i>	<i>P</i> 2 ₁ / <i>c</i>	<i>P</i> $\bar{1}$	<i>P</i> 2 ₁ / <i>c</i>	<i>P</i> 2 ₁ / <i>n</i>	<i>P</i> 2 ₁ / <i>c</i>
<i>a</i> (Å)	11.971(5)	6.581(5)	10.6405(18)	12.125(2)	13.975(14)	12.8234(7)
<i>b</i> (Å)	6.692(3)	21.472(17)	12.712(2)	7.2540(14)	6.227(7)	6.9230(4)
<i>c</i> (Å)	17.466(8)	7.066(5)	16.534(3)	12.888(2)	15.099(16)	12.7631(7)
<i>α</i> (deg)	90.00	90.00	107.075(4)	90.00	90.00	90.00
<i>β</i> (deg)	108.810(8)	104.36(2)	97.638(3)	97.581(5)	115.12(2)	111.8740(10)
<i>γ</i> (deg)	90.00	90.00	105.029(4)	90.00	90.00	90.00
<i>V</i> (Å ³)	1324.3(10)	967.2(13)	2056.8(6)	1123.7(4)	1190(2)	1051.49(10)
<i>Z</i>	4	4	6	4	4	4
<i>R</i> ₁ (> 2σ(<i>I</i>))	0.0547	0.0682	0.0760	0.0958	0.0426	0.0377
wR ₂ (all data)	0.1627	0.1977	0.2317	0.2829	0.1275	0.1095
CCDC No.	1448262	1448265	1448263	1448264	1448260	1448261

Table S3. Thermal properties including melting point (T_m) and initial weight-loss temperature (T_i) of BPMI, DBPI, DPPI, and PMI-(II).

Compound	T_m/T_i ($^{\circ}\text{C}$)
BPMI	203/261
DBPI	180/256
DPPI	219/260
PMI-(II)	190/259

Table S4. Hydrogen bonds for PDI [\AA and deg.].

D-H...A	d(D-H)	d(H...A)	d(D...A)	<(DHA)
C(17)-H(17B)...O(2)#1	0.99	2.51	3.376(18)	145

Symmetry transformations used to generate equivalent atoms:

#1 $x, y-1, z$

Table S5. Hydrogen bonds for PTI [\AA and deg.].

D-H...A	d(D-H)	d(H...A)	d(D...A)	<(DHA)
C(5)-H(5)...O(2)#1	0.95	2.54	3.231(3)	130

Symmetry transformations used to generate equivalent atoms:

#1 $x, -y+1, z-1/2$

Table 6. Hydrogen bonds for PMI-(I) [\AA and deg.].

D-H...A	d(D-H)	d(H...A)	d(D...A)	<(DHA)
C(6)-H(6)...O(2)#1	0.95	2.54	3.211(3)	128

Symmetry transformations used to generate equivalent atoms:

#1 $x, -y+1, z+1/2$